Chapter 1
The method of fundamental solutions for computing interior transmission eigenvalues of inhomogeneous media

L. Pieronek and A. Kleefeld

Abstract The method of fundamental solutions is applied to the approximate computation of interior transmission eigenvalues for a special class of inhomogeneous media in two dimensions. We give a short approximation analysis accompanied with numerical results that clearly prove practical convenience of our alternative approach.

1.1 Introduction

The interior transmission eigenvalue problem (ITEP) arises in the study of inverse scattering problems as a precursor to justify the feasibility of quantitative reconstruction methods, see [CaHa12]. The corresponding eigenvalues (ITEs) are associated with certain critical wave numbers which allow for incident test waves with arbitrary small scattering responses that would hardly be detected in experiments. One can prove in a mathematically rigorous way, see [KiGr08], that this loss of information due to the scatterer's practical invisibility indeed complicates its recovery process on the basis of sampling methods, for example.

While it has been known for quite a long time that ITEs fortunately only form an at most discrete set, their accurate computation for a given scatterer is still rather challenging since the underlying ITEP is both non-elliptic and non-selfadjoint. In this paper, we will present a relatively easy algorithm for the efficient approximation of ITEs using a robust version of the method of fundamental solutions (MFS). Having thus been positively tested for perfectly homogeneous and possibly anisotropic

L. Pieronek
Forschungszentrum Jülich GmbH, 52425 Jülich, Germany,
e-mail: l.pieronek@fz-juelich.de

A. Kleefeld
Forschungszentrum Jülich GmbH, 52425 Jülich, Germany,
e-mail: a.kleefeld@fz-juelich.de

scatterers so far, see [KlPi18a] and [KlPi18b], we will now analyze and reinvestigate the numerical merits of the method in the generalized context of inhomogeneous media that decompose into several homogeneities stuck in a surrounding bulk. For competitive alternative methods in this context, see the solution of the direct problem in [GiPa13], for example.

1.2 The ITEP and the modified MFS

Let $D \subset \mathbb{R}^2$ be a bounded and simply connected domain with smooth boundary representing the contour of some scatterer. According to our modeling assumptions, there exists an upper component number $1 \leq N_c \in \mathbb{N}$ and a disjoint decomposition $\bigcup_{i=1}^{N_c} D_i \subset D \subset \overline{D} = \bigcup_{i=1}^{N_c} \overline{D_i}$ of homogeneous composites such that the D_i are each open, connected and fulfill for $i_1 \neq i_2$ either $\partial D_{i_1} \cap \partial D_{i_1} = \emptyset$ or $\partial D_{i_1} \cap \partial D_{i_1}$ being a smooth and non-intersecting closed contour. Besides, we assume the existence of some bulk which will be emphasized by D_1 and which distinguishes from the other components through its surrounding property $\partial D \subset \partial D_1$ unlike $\partial D \cap \partial D_i = \emptyset$ for $2 \leq i \leq N_c$, cf. Figure 1.1. As such, D may be considered as an inner pollution of the original material D_1 by the components D_i for $i > 2$. These different material parameters will be reflected via piecewise-constant functions on D with jumps only across ∂D_i and encompass the index of refraction $n \in L^\infty(D, \mathbb{R}_{>0})$, as a local measure for the propagation speed of the penetrable wave under consideration, and the diffusivity tensor $A \in L^\infty(D, \mathbb{R}^{2\times 2}_{sym})$ to reflect the material's anisotropic structure, if necessary (otherwise set $A = I$, where I denotes the identity matrix in $\mathbb{R}^2$). Depending on whether $A = I$ on D or not, there are also mathematical constraints for n and the eigenvalues of A that we will specify later. When focusing on the analysis of each homogeneous component, we also write $f_i := f_{|D_i}$ for any function f on D.

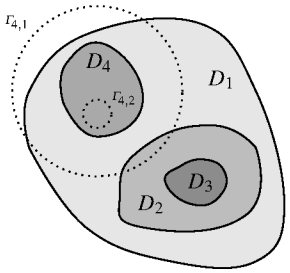

Fig. 1.1 Exemplary scatterer D with bulk D_1 that contains three inner components D_2, D_3, D_4. For demonstration purposes, some admissible source boundary $\Gamma_4 = \Gamma_{4,1} \cup \Gamma_{4,2}$ for D_4 is added dottedly in the component's outside and inside, respectively.

In contrast to inverse problems, we assume all these material data to be known a priori and want to compute ITEs on that basis in the following. An ITE is a wave

number $k > 0$ for which the ITEP

$$\begin{aligned} \operatorname{div}(A\nabla w) + k^2 n w &= 0 \quad \text{in } D\,, \\ \Delta v + k^2 v &= 0 \quad \text{in } D\,, \\ w &= v \quad \text{on } \partial D\,, \\ \partial_{\nu_A} w &= \partial_\nu v \quad \text{on } \partial D\,, \end{aligned} \tag{1.1}$$

where ν_A denotes the (co-)normal derivative, can be solved appropriately in a non-trivial way. The penultimate condition refers to the regularity assumptions of admissible eigenfunctions being $(v,w) \in L^2(D)$ with $(v-w) \in H_0^2(D)$ for the isotropic case and $(v,w) \in H^1(D)$ otherwise. The origin for such a differentiation is that the usual Fredholm setting approved for eigenvalue investigations can at most be guaranteed then.

Having settled a proper abstract framework for such a non-linear eigenvalue problem, approximations of ITEs can be obtained as a byproduct of finite dimensional approximation of the corresponding eigenfunctions. The standard MFS achieves this for homogeneous media by looking for superposed trial functions that are translations of certain fundamental solutions from the governing PDE. This ansatz is somewhat converse to finite element methods as each solution candidate automatically fulfills the interior conditions of (1.1) exactly, but not necessarily the prescribed boundary conditions along ∂D, cf. [GiPa13]. However, since we actually work with scatterers that are piecewise-homogeneous, we want to apply this method at least locally for each composite and properly supported trial functions. This then requires additional control of function transitions across adjacent components D_j and D_i according to our globally imposed regularity assumptions of exact eigenfunctions. Fortunately, these extra costs only affect the approximation of w since v always obeys a pure Helmholtz equation with constant wave number so that its trial functions can still be defined throughout D. These observations finally make us consider the following MFS-based approximation spaces of order m. For v, we set

$$V_m := \operatorname{span}\{\phi_1^v, \ldots, \phi_m^v\}\,,$$

where

$$\phi_r^v(x) := \frac{\mathrm{i}}{4} H_0^{(1)}(k|x - s_r^v|)\,,$$

$H_0^{(1)}$ is the first Hankel function of order zero, $x \in \overline{D}$ is the actual argument whereas $\{s_1^v, \ldots, s_m^v\}$ are the so-called source points for v which have to lie on some closed exterior contour Γ^v disjoint to D. For w, we need to take into account the refined treatment of the domain and define an artificial boundary for each composite in its individual exterior. Since the D_i are in general multiply-connected, each of the $N_e(i)$ enclaves E_{i,j_i} of $\mathbb{R}^2 \setminus \overline{D}_i$ are labeled by j_i, always starting with the unbounded component by convention. Then we endow each of them with their own closed contour $\Gamma_{i,j_i}^w \Subset E_{i,j_i}$ and wish to choose $\Gamma_{1,j_1}^w = \Gamma^v$. We may thus drop the superscripts w or

v from now and abbreviate the union over j_i for all assigned source contours Γ_{i,j_i} of D_i by Γ_i. We can finally setup the approximation space W_m as the span of

$$\phi^w_{i,j_i,r}(x) := \frac{\mathrm{i}}{4\det A_i^{\frac{1}{2}}} H_0^{(1)}\left(\sqrt{n_i}k\left|A_i^{-\frac{1}{2}}\left(x - s^w_{i,j_i,r}\right)\right|\right)\mathbb{1}_{\overline{D}_i}\ ,$$

where $s^w_{i,j_i,r}$ are now the source points for w on Γ^w_{i,j_i} with $1 \le r \le m$. Thus the dimension of W_m is actually a multiple of m depending on the number of composites N and of their actual voids.

The optimal MFS solution pair $(v_m, w_m) \in V_m \times W_m$ then tries to fulfill both the boundary conditions of the ITEP (1.1) and the transitional regularity criteria for global eigenfunctions best in the sense of a minimal collocation error. Therefore we select representative points $\{x_{i_1,i_2,1},\ldots,x_{i_1,i_2,m}\}$ along the interface of $\partial D_{i_1} \cap \partial D_{i_2}$ where $0 \le i_1 < i_2 \le N_c$ and $D_0 := \mathbb{R}^2\backslash\overline{D}$ is introduced for simplicity. We implicitly omit the definition of those $x_{i_1,i_2,\ell} \in D$ whose pair (i_1,i_2) would be associated with an empty intersection. The same convention will affect all the x_{0,i_2} with $i_2 > 1$ due to the separating bulk. Again, the total number of collocation points is a multiple of m, but this time depending on the cumulated number of boundaries of all the D_i.

Instead of performing the collocation procedure now in a straightforward way that would result in a numerically ill-conditioned problem, we follow the stabilization improvement from Betcke and Trefethen, see [BeTr05], that also gives rise to call our corresponding MFS update the *modified MFS* henceforth. For that we pick m-independent auxiliary points $\{a_1,\ldots,a_{N_a}\}$ from $\bigcup_{i=1}^{N_c} D_i$ which will later ensure that our approximations of eigenfunctions are sufficiently large in the interior. Thus the utterly critical zero function will never be detected as a theoretically admissible (with respect to (1.1)), but practically undesirable solution candidate.

Let us structure this amount of introduced data in matrix form to see more easily how they emerge in the modified MFS collocation procedure. If (i_1,i_2) is a feasible pair such that $\partial D_{i_1} \cap \partial D_{i_2} \neq \emptyset$, we define $W_{i_1,i_2,i,j_i} \in \mathbb{C}^{2m\times m}$ parametrized by $1 \le i \le N_c$ and $0 \le i_1 < i_2 \le N_c$ for the varyingly supported trial functions of W_m via

$$\begin{aligned}(W_{i_1,i_2,i,j_i})_{\ell,r} &:= \phi^w_{i,j_i,r}(x_{i_1,i_2,\ell})\ ,\\ (W_{i_1,i_2,i,j_i})_{m+\ell,r} &:= \partial_\nu \phi^w_{i,j_i,r}(x_{i_1,i_2,\ell})\ ,\end{aligned}$$

whereas for V_m it suffices to consider $V \in \mathbb{C}^{2m\times m}$ given by

$$\begin{aligned}(V)_{\ell,r} &:= \phi^v_r(x_{0,1,\ell})\ ,\\ (V)_{m+\ell,r} &:= \partial_\nu \phi^v_r(x_{0,1,\ell})\ .\end{aligned}$$

Here, $1 \le \ell, r \le m$ and ν is a unit normal vector along $\partial D_{i_1} \cap \partial D_{i_2} \neq \emptyset$ pointing in the same direction for both components D_{i_1} and D_{i_2}. The evaluations of trial functions at interior points are summarized in an analogical fashion to matrices in $\mathbb{C}^{N_a\times m}$ and read

$$(\widetilde{W}_{i,j_i})_{\ell,r} := \phi^w_{i,j_i,r}(a_\ell)$$

as well as

$$(\widetilde{V})_{\ell,r} := \phi_r^v(a_\ell) \ ,$$

respectively. In the anisotropic case, $\widetilde{W}_{i,j}$ and $\widetilde{V}$ may even be extended to matrices in $\mathbb{C}^{3N_a \times m}$ by attaching corresponding partial derivative evaluations of $\phi^w_{i,j_i,r}$ and ϕ^v_r, respectively, for being more consistent with the norms introduced in the abstract setting later. Through this matrix reformulation, the m-independent indices i_1, i_2, i, j_i for the different scattering composites are separated from the m-dependent point discretizations labeled by ℓ, r. Since their matrices are implicitly parametrized by the wave number k, we finally define the block-type system $T(k)$ by

$$T(k) := \begin{pmatrix} V & W_{0,1,1,1} & \dots & W_{0,1,1,N_e(1)} & 0 & \dots\ \dots & 0 \\ 0 & W_{1,2,1,1} & \dots & W_{1,2,1,N_e(1)} & W_{1,2,2,1} & \dots\ \dots & W_{1,2,N_c,N_e(N_c)} \\ \vdots & \vdots & & \vdots & \vdots & & \vdots \\ \vdots & \vdots & & \vdots & \vdots & & \vdots \\ 0 & W_{N_c-1,N_c,1,1} & \dots & W_{N_c-1,N_c,1,N_e(1)} & W_{N_c-1,N_c,2,1} & \dots\ \dots & W_{N_c-1,N_c,N_c,N_e(N_c)} \\ \widetilde{V} & 0 & \dots & \dots & \dots & \dots\ \dots & 0 \\ 0 & \widetilde{W}_{1,1} & \dots & \widetilde{W}_{1,N_e(1)} & \widetilde{W}_{2,1} & \dots\ \dots & \widetilde{W}_{N_c,N_e(N_c)} \end{pmatrix} .$$

Recall that the majority of the W matrices are zero since not all components D_{i_1} and D_{i_2} will be adjacent, i.e. $W_{i_1,i_2,i,j_i} = 0 \in \mathbb{C}^{m\times m}$ if $i \notin \{i_1, i_2\}$. This might motivate to treat T in parallel from a programming perspective, especially because the last technical thing left to do is performing a QR factorization of $T(k) = Q_T(k)R_T(k)$. Extracting its unitary part, we may write

$$Q_T(k) = \begin{pmatrix} Q(k) \\ \widetilde{Q}(k) \end{pmatrix} \ .$$

Similar as above, $\widetilde{Q}(k)$ corresponds to the lower $2N_a$ scalar rows whereas $Q(k)$ comprises the remaining upper part of $Q_T(k)$. Such a decomposition of $Q_T(k)$ and thus of $T(k)$ will implicitly help us later to distinguish numerically between real and spurious eigenvalue approximations in an effective way.

Now we have everything together to formulate our approximate ITEP based on the modified MFS in a very compact form: Find those k for which $k \mapsto Q(k)$ is almost singular. For this purpose, the smallest singular value $\sigma_1(k)$ of $Q(k)$ will serve as a convenient measure for the degeneracy of $Q(k)$ whenever its magnitude is close to zero. Corresponding wave numbers will be called approximate ITEs and will be denoted by k_m to relate its dimensional origin to the underlying eigenfunction approximation. In the next section we will discuss our derived approach from a more abstract perspective and show its feasibility in practice.

1.3 Approximation analysis

The major difference for the application of the modified MFS between purely and piecewise homogeneous media is apparently the additional treatment of interior composite transitions for w. So far we take them numerically into account by pointwise collocation, but is seems more natural to formulate precise assumptions with respect to their original Sobolev spaces. Therefore we focus on $N_c > 1$ in the sequel and assume first that $A = I$, i.e. the scatterer is entirely isotropic. Then the corresponding ITEP eigenfunctions are only in $L^2(D)$, in particular the w-dependent PDE has to be fulfilled in a distributional sense and reads

$$\int_D (\Delta\psi + k^2 n\psi) w \,\mathrm{d}x = 0$$

for any $\psi \in C_c^\infty(D)$. If we now approximate w by some proper $w_m \in W_m$, the integral above does not vanish any more for all test functions in general. However, choosing $\psi \in C_c^\infty(D \setminus \bigcup_{i \neq i_1,i_2} \overline{D}_i) \subset C_c^\infty(D)$, where $1 \leq i_1 < i_2 \leq N_c$ are some adjacent component indices, the following reformulation shows that the resulting deviations are completely due to certain integral misfits over $\partial D_{i_1} \cap \partial D_{i_2}$. This is because our the trial functions in W_m, although they solve the corresponding interior ITEP condition pointwise almost everywhere, are a priori discontinuous along composite transitions:

$$\begin{aligned}
&\int_D (\Delta\psi + k^2 n\psi) w_m \,\mathrm{d}x \\
&= \int_{D_{i_1}} (\Delta\psi + k^2 n_{i_1}\psi) w_{m,i_1} \,\mathrm{d}x + \int_{D_{i_2}} (\Delta\psi + k^2 n_{i_2}\psi) w_{m,i_2} \,\mathrm{d}x \\
&= \int_{\partial D_{i_1} \cap \partial D_{i_2}} \partial_\nu \psi (w_{m,i_1} - w_{m,i_2}) - \psi \partial_\nu (w_{m,i_1} - w_{m,i_2}) \,\mathrm{d}s \\
&+ \int_{D_{i_1}} \underbrace{(\Delta w_{m,i_1} + k^2 n_{i_1} w_{m,i_1})}_{=0} \psi \,\mathrm{d}x + \int_{D_{i_2}} \underbrace{(\Delta w_{m,i_2} + k^2 n_{i_2} w_{m,i_2})}_{=0} \psi \,\mathrm{d}x \\
&= \int_{\partial D_{i_1} \cap \partial D_{i_2}} \partial_\nu \psi (w_{m,i_1} - w_{m,i_2}) - \psi \partial_\nu (w_{m,i_1} - w_{m,i_2}) \,\mathrm{d}s \,.
\end{aligned} \tag{1.2}$$

Conversely, we hope to recover some exact eigenfunction w with $w, \Delta w \in L^2(D)$ in the limit $m \to \infty$, so we expect $(w_{m,i_1} - w_{m,i_2})$ to be evanescent at least with respect to $H^{-\frac{1}{2}}(\partial D_{i_1} \cap \partial D_{i_2})$ and likewise $\partial_\nu (w_{m,i_1} - w_{m,i_2})$ should be controlled as $H^{-\frac{3}{2}}(\partial D_{i_1} \cap \partial D_{i_2})$-traces. However, for technical reasons that will become clear later, we assume the convergence to hold more strongly in $H^{\frac{3}{2}}(\partial D_{i_1} \cap \partial D_{i_2})$ and $H^{\frac{1}{2}}(\partial D_{i_1} \cap \partial D_{i_2})$, respectively. In the anisotropic case, however, we can stay with the natural approximation assumptions $(w_{m,i_1} - w_{m,i_2}) \to 0$ in $H^{\frac{1}{2}}(\partial D)$ and $(\partial_{\nu_{A_{i_1}}} w_{m,i_1} - \partial_{\nu_{A_{i_2}}} w_{m,i_2}) \to 0$ in $H^{-\frac{1}{2}}(\partial D)$ that originate from $w \in H^1(D)$.

In order to finally adapt the prescribed boundary conditions on ∂D of the eigenfunctions from (1.1) in our approximation procedure, the explicit regularity conditions on $(v-w)$ need to be taken into account. Accordingly, the isotropic case asserts $(v-w) \in H_0^2(D)$ which suggests imposing $(v_m - w_m) \to 0$ in $H^{\frac{3}{2}}(\partial D)$ as well as $\partial_\nu(v_m - w_m) \to 0$ in $H^{\frac{1}{2}}(\partial D)$ by continuity of the corresponding trace operators. In the anisotropic case we similarly arrive at $(v_m - w_m) \to 0$ in $H^{\frac{1}{2}}(\partial D)$ and $(\partial_\nu v_m - \partial_{\nu_A} w_m) \to 0$ in $H^{-\frac{1}{2}}(\partial D)$.

Altogether, these preliminaries are to show that the analysis of the ITEP based on the modified MFS (embedded into the abstract setting) is conceptually the same for undiluted and piecewise homogeneous media. Therefore we expect most of the results from [KlPi18a] and [KlPi18b] to be extendable to our specially inhomogeneous setting such as the following theorem. It can be considered as the justification for the applicability of the modified MFS to ITE approximations.

Theorem 1. *Consider a sequence $\{(v_m, w_m, k_m)\}_{m\in\mathbb{N}} \subset V_m \times W_m \times \mathbb{R}_{>0}$ for either $A = I$ with restriction $n > 1$ or $n < 1$ throughout D, $0 < A < I$ or $I < A$ (where the matrix order is understood with respect to positive definiteness) which fulfills the following properties, respectively:*
In the isotropic case, we assume

1. *eigenvalue convergence: $k_m \to k \neq 0$,*
2. *uniform interior bounds: $C^{-1} < \left(\|v_m\|^2_{L^2(D)} + \|w_m\|^2_{L^2(D)}\right) < C$ for some $C > 1$ and for all m large enough,*
3. *vanishing boundary data: $\left(\|v_m - w_m\|_{H^{\frac{3}{2}}(\partial D)} + \|\partial_\nu(v_m - w_m)\|_{H^{\frac{1}{2}}(\partial D)}\right) \to 0$ & $\left(\|w_{m,i_1} - w_{m,i_2}\|_{H^{\frac{3}{2}}(\partial D_{i_1} \cap \partial D_{i_2})} + \|\partial_\nu(w_{m,i_1} - w_{m,i_2})\|_{H^{\frac{1}{2}}(\partial D_{i_1} \cap \partial D_{i_2})}\right) \to 0$ for adjacent components $D_{i_1}, D_{i_2} \subset D$,*

whereas in the anisotropic case, the corresponding assumptions read

1.' *eigenvalue convergence: $k_m \to k \neq 0$,*
2.' *uniform interior bounds: $C^{-1} < \left(\|v_m\|^2_{H^2(D)} + \|w_m\|^2_{H^2(D)}\right) < C$ for some $C > 1$ and for all m large enough,*
3.' *vanishing boundary data: $\left(\|v_m - w_m\|_{H^{\frac{1}{2}}(\partial D)} + \|\partial_\nu v_m - \partial_{\nu_A} w_m\|_{H^{-\frac{1}{2}}(\partial D)}\right) \to 0$ & $\left(\|w_{m,i_1} - w_{m,i_2}\|_{H^{\frac{1}{2}}(\partial D_{i_1} \cap \partial D_{i_2})} + \|\partial_{\nu_{A_{i_1}}} w_{m,i_1} - \partial_{\nu_{A_{i_2}}} w_{m,i_2}\|_{H^{-\frac{1}{2}}(\partial D_{i_1} \cap \partial D_{i_2})}\right) \to 0$ for adjacent components $D_{i_1}, D_{i_2} \subset D$.*

In either case, the limit k of the approximate eigenvalues k_m is an ITE.

Proof. Since our proof to be presented works structurally similar for the anisotropic case based on the corresponding techniques from the homogeneous scenario, see [KlPi18b], but much easier due to more consistent control assumptions of (v_m, w_m) throughout $\overline{D}$, see condition 3', we only focus on the isotropic case in the following.

We aim to construct an eigenfunction candidate (v,w) and show that it fulfills the required properties for k being a real ITE. We take the weak $L^2(D)$-limit of our

approximate pairs (v_m, w_m) which exists (actually only for a subsequence which we will, however, not explicitly restate in the sequel) by weak compactness and the uniform bounds provided in assumption 2. The fact that v is then a distributional solution of the Helmholtz equation on D is quite trivial because it can be shown exactly as in the homogeneous case. The corresponding result for w relies on an additional treatment of (1.2) *which is then also straightforward by condition 3. So far, we therefore know that $(v,w) \in L^2(D) \times L^2(D)$ fulfills the interior conditions of* (1.1) *and we want to prove next that $u := (v-w) \in H_0^2(D)$, i.e. u has zero boundary data and is twice weakly differentiable in the interior (the latter criterion would be redundant for the anisotropic demonstration).*

We modify the piecewise smooth but generally discontinuous difference functions $u_m := (v_m - w_m) \in L^2(D)$ to $\widetilde{u}_m \in H^2(D)$ that will be uniformly bounded with respect to m. As potential jumps of u_m go back to those of w_m across ∂D_i for $i > 1$, we want to fill these discontinuity gaps by adding certain lifting functions $\theta_{m,i} \in H^2(D_i)$ to u_m. More precisely, we set for $i > 1$

$$\begin{aligned} \Delta^2 \theta_{m,i} &= 0 \quad \text{in } D_i \ , \\ \theta_{m,i} &= (w_{m,i^*} - w_{m,i}) \mathbb{1}_{\partial D_i \cap \partial E_{i,1}} \quad \text{on } \partial D_i \ , \\ \partial_\nu \theta_{m,i} &= \partial_\nu (w_{m,i^*} - w_{m,i}) \mathbb{1}_{\partial D_i \cap \partial E_{i,1}} \quad \text{on } \partial D_i \ , \end{aligned}$$

where $1 \le i^* \le N_c$ is determined uniquely by $D_{i^*} \subset \partial E_{i,1}$ and $\partial D_i \cap \partial D_{i^*} \neq \emptyset$. Then we extend $\theta_{m,i}$ by zero in $D \backslash D_i$. Standard a priori estimates ensure that our lifting functions can be bounded within their support D_i by

$$\|\theta_{m,i}\|_{H^2(D_i)} \le C \left(\|w_{m,i} - w_{m,i^*}\|_{H^{\frac{3}{2}}(\partial D_i \cap \partial D_{i^*})} + \|\partial_\nu (w_{m,i} - w_{m,i^*})\|_{H^{\frac{1}{2}}(\partial D_i \cap \partial D_{i^*})} \right)$$

and globally they cumulate by definition to

$$\widetilde{u}_m := u_m + \sum_{i=2}^{N_c} \theta_{m,i} \ \in H^2(D) \ .$$

Therefore, $\widetilde{u}_m$ solves

$$\begin{aligned} \Delta \widetilde{u}_m &= -k_m (v_m - n w_m) + \sum_{i=2}^{N_c} \Delta \theta_{m,i} \quad \text{in } D_i \ , \\ \widetilde{u}_m &= v_m - w_m \quad \text{on } \partial D_i \ , \\ \partial_\nu \widetilde{u}_m &= \partial_\nu (v_m - w_m) \quad \text{on } \partial D_i \ , \end{aligned}$$

and is bounded by

$$\|\widetilde{u}_m\|_{H^2(D)} \le C \left(\|\Delta \widetilde{u}_m\|_{L^2(D)} + \|v_m - w_m\|_{H^{\frac{3}{2}}(\partial D)} + \|\partial_\nu (v_m - w_m)\|_{H^{\frac{1}{2}}(\partial D)} \right) \ .$$

In particular, the $\widetilde{u}_m$ converge both weakly in $H^2(D)$ and strongly in $L^2(D)$. Since $\theta_{m,i} \to 0$, the strong $L^2(D)$-limit of u_m and $\widetilde{u}_m$ coincide which then implies that $u \in H^2(D)$. The fact that even $u \in H_0^2(D)$ finally follows by assumption 3 and the continuity of the trace operators from $H^2(D)$ to $H^{\frac{3}{2}}(\partial D)$ and to $H^{\frac{1}{2}}(\partial D)$, respectively.

It remains to prove that $u \neq 0$. We will contrarily assume that $u = 0$ which would then imply $u_m \to 0$ in $L^2(D)$ according to our previous derivations. Expanding the $L^2(D)$-norm in its scalar product representation, we may conclude, including assumption 2

$$\begin{aligned}\liminf_{m\to\infty} \operatorname{Re} \int_D v_m \overline{w}_m \,\mathrm{d}x &= \liminf_{m\to\infty} \frac{1}{2}\left(\|v_m\|^2_{L^2(D)} + \|w_m\|^2_{L^2(D)} - \|v_m - w_m\|^2_{L^2(D)}\right) \\ &= \liminf_{m\to\infty} \frac{1}{2}\left(\|v_m\|^2_{L^2(D)} + \|w_m\|^2_{L^2(D)}\right) \geq \frac{1}{2C} > 0\,.\end{aligned}$$

Determined by keeping positive signs above, we multiply the latter inequality either with $(1-n_i)$ or with $(n_i - 1)$, assuming the latter without loss of generality. Since $\min_{1\leq i\leq N_c}(n_i - 1) > 0$ and $k_m \to k > 0$, we thus obtain

$$\begin{aligned}0 &< \liminf_{m\to\infty} \operatorname{Re} \int_D k_m^2 (n_i - 1) v_m \overline{w}_m \,\mathrm{d}x \\ &= \liminf_{m\to\infty} \operatorname{Re} \int_D \overline{w}_m \Delta v_m - v_m \Delta \overline{w}_m \,\mathrm{d}x \\ &= \liminf_{m\to\infty} \operatorname{Re} \int_{\partial D} \overline{w}_m \partial_\nu v_m - v_m \partial_\nu \overline{w}_m \,\mathrm{d}s \\ &= \liminf_{m\to\infty} \operatorname{Re} \int_{\partial D} \overline{w}_m \partial_\nu v_m - \overline{v}_m \partial_\nu v_m + v_m \partial_\nu \overline{v}_m - v_m \partial_\nu \overline{w}_m \,\mathrm{d}s \\ &= \liminf_{m\to\infty} \operatorname{Re} \int_{\partial D} (\overline{w}_m - \overline{v}_m) \partial_\nu v_m + v_m \partial_\nu (\overline{v}_m - \overline{w}_m) \,\mathrm{d}s \\ &\leq \liminf_{m\to\infty} \|v_m - w_m\|_{H^{\frac{3}{2}}(\partial D)} \|v_m\|_{H^{-\frac{3}{2}}(\partial D)} + \|\partial_\nu v_m\|_{H^{-\frac{1}{2}}(\partial D)} \|\partial_\nu (v_m - w_m)\|_{H^{\frac{1}{2}}(\partial D)} \\ &= 0\,.\end{aligned} \tag{1.3}$$

The last equality follows by assumption 3 and by some uniform upper bound on the negative dual norms as inherited from our interior control of v_m, cf. assumption 2. Obviously, (1.3) *gives a contradiction and manifests that $u \neq 0$ which thus completes the proof.*

Remark: The proof above indicates why our initial modeling assumptions for D restrict to material components D_i facing never more than one another at each transitional point. Otherwise, the traces of different w_m parts might be incompatible in any crossing point which would then lock the possibility to find sufficiently regular lifting functions in its vicinity.

1.4 Numerical examples

In this section we use the modified MFS to compute the first four real ITEs for the unit disc D varied in two different inner configurations. One of the two, let us say $D^{\circ\circ}$, will have separated disc-shaped components, while for the other we choose a corresponding concentric composition and denote it by $D^{\circledcirc}$, cf. Figure 1.2. More concretely, we analyzed three-components-scatterers whose set representation decompose into

$$D_2^{\circ\circ} := B_{0.4}\big((0.5,0)\big)\,, \quad D_3^{\circ\circ} := B_{0.3}\big((-0.5,0)\big)\,, \quad D_1^{\circ\circ} := B_1\big((0,0)\big)\backslash(D_2^{\circ\circ}\cup D_3^{\circ\circ})$$

and

$$D_2^{\circledcirc} := B_{0.4}\big((0,0)\big)\,, \quad D_3^{\circledcirc} := B_{0.3}\big((0,0)\big)\,, \quad D_1^{\circledcirc} := B_1\big((0,0)\big)\backslash(D_2^{\circledcirc}\cup D_3^{\circledcirc})\,,$$

respectively. Here, $B_r(c)$ denotes the disc of radius r centered at $c\in\mathbb{R}^2$. We equipped $D^{\circledcirc}$ and $D^{\circ\circ}$ each with some identical sample of refractive indices for both the isotropic and anisotropic case which read $n_1=4, n_2=3, n_3=2$ and set additionally for $A\neq I$

$$A_1=\begin{pmatrix}2&0\\0&4\end{pmatrix}\,, \quad A_2=\begin{pmatrix}3&0\\0&2\end{pmatrix}\,, \quad A_3=\begin{pmatrix}2&0\\0&3\end{pmatrix}\,.$$

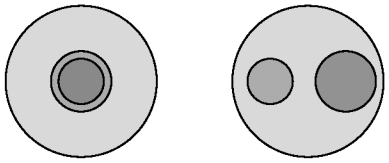

A	D	ITE 1	ITE 2	ITE 3	ITE 4
$=I$	$D^{\circledcirc}$	3.3472649097009	3.5339744459219	3.8215531039714	4.0276794096285
	$D^{\circ\circ}$	2.9695607637622	3.8151728473562	4.2620616635742	4.3612725527356
$\neq I$	$D^{\circledcirc}$	1.143183893	1.64497010	2.443821	3.273054
	$D^{\circ\circ}$	1.2372795	1.569690	2.261430	3.1939135

Fig. 1.2 Visualization of the scatterers $D^{\circledcirc}$ (left) and $D^{\circ\circ}$ (right) and listing of their first four real ITEs both for the isotropic ($=I$) and anisotropic case ($\neq I$) with common index of refraction given by $n_1=4, n_2=3, n_2=2$.

Having thus fixed our material parameters, there is now much freedom in choosing the computational points for the modified MFS procedure. First of all, we associated source boundaries $\Gamma_i^{\circledcirc}$ and $\Gamma_i^{\circ\circ}$ to the components of $D_i^{\circledcirc}$ and $D_i^{\circ\circ}$, respectively, by scaling the underlying circles with respect to their individual center by some factor $S=1.5>1$ for the outer part of the source boundary, cf. $\Gamma_{i,1}^{\circledcirc}$ and $\Gamma_{i,1}^{\circ\circ}$, and

similarly by $s = 0.5 < 1$ for the remaining ones, if required. Therefore we arrive at

$$\begin{aligned}
&\Gamma_{1,1}^{\circ\circ} := \partial B_S\big((0,0)\big)\ , \quad \Gamma_{1,2}^{\circ\circ} := \partial B_{0.4s}\big((0.5,0)\big)\ , \quad \Gamma_{1,3}^{\circ\circ} := \partial B_{0.3s}\big((-0.5,0)\big)\ ,\\
&\Gamma_{2,1}^{\circ\circ} := \partial B_{0.4S}\big((0.5,0)\big)\ ,\\
&\Gamma_{3,1}^{\circ\circ} := \partial B_{0.3S}\big((-0.5,0)\big)\ ,
\end{aligned}$$

for $D^{\circ\circ}$ and

$$\begin{aligned}
&\Gamma_{1,1}^{\circledcirc} := \partial B_S\big((0,0)\big)\ , \quad \Gamma_{1,2}^{\circledcirc} := \partial B_{0.4s}\big((0,0)\big)\ ,\\
&\Gamma_{2,1}^{\circledcirc} := \partial B_{0.4S}\big((0,0)\big)\ , \quad \Gamma_{2,2}^{\circledcirc} := \partial B_{0.3s}\big((0,0)\big)\ ,\\
&\Gamma_{3,1}^{\circledcirc} := \partial B_{0.3S}\big((0,0)\big)\ ,
\end{aligned}$$

for $D^{\circledcirc}$. Since the location of interior points turns out not to contribute significantly to the output, we placed them also on a circle with identical center as $D_3^{\circledcirc}$ and $D_3^{\circledcirc}$, respectively, but half its radius. Conveniently, all the computational points introduced in the second section of this paper could thus be distributed equidistantly on their corresponding circles.

In the process of our numerical experiments, we fixed $N_a = 10$ and varied m to improve the accuracy of our approximate ITEs. Minimizing the first singular value, the optimal results from Figure 1.2 were achieved for $60 \leq m \leq 100$ and thus at most 500 collocation points were needed altogether. Exceeding this regime leads more and more to the emergence of ill-conditioning effects and thus to unreliable results. However, approaching the admissible threshold for m from below, the cut-off mantissa of our ITEs approximations tend to converge with increasing m, so we believe all the listed digits to be correct (modulo round-off-errors). Note that due to the rotational-invariant structure of $D^{\circledcirc}$ at least in the case $A = I$ all ITEs can easily be computed analytically using a Fourier Bessel ansatz, cf. [KlPi18a] with a correspondingly extended matrix system for the component transitions of v and w. The first four of them were found to be 3.347264909700945, 3.533974445921942, 3.821553103971393, 4.027679409628525 and thus confirm that the approximations obtained by the modified MFS are indeed correct up to machine precision here.

Generally, our current observations are mostly consistent with those made for purely homogeneous scatterers, see the references [KlPi18a] and [KlPi18b]. In particular, the computational results from the isotropic case are still significantly better than for $I \neq A$ which goes back to the more advanced body of trial functions for w. Novelties affect the irregular behavior of the smallest singular value function whose minimal dips were sometimes extremely steep and thus hard to detect (such as the largest eigenvalue given above that was recomputed with the Fourier Bessel ansatz). As an explanation for that, the optimal number of collocation points necessary for the transitional boundaries to preserve a comparable quality of eigenvalue approximations turned out to be surprisingly large. While the undiluted isotropic disc required only around $m = 20$ collocation points altogether to recover ITEs almost up to machine precision, our latest experiments necessitate almost about its fivefold per boundary component (500 in total) and thus seem to scale quadratically.

1.5 Conclusion

In this paper, the recovery of interior transmission eigenvalues for inhomogeneous media in two dimensions was investigated on the basis of the method of fundamental solutions. Although best suited for homogeneous scatterers to benefit most from the lower dimensional boundary description, our numerical examples show that highly accurate results can still be obtained for scatterers which consist of a moderate number of homogeneous components. Conversely, the more complex the inner structure of D is, including anisotropic behavior, the more collocation points are generally needed and in correlation with that the less precise the eigenvalue approximation becomes. Our theoretical studies additionally show that our method will, under appropriate assumptions of the output, never detect spurious eigenvalues in the limiting process and thus proves its practical reliability.

References

[BeTr05] Betcke, T. and Trefethen, L. N.: Reviving the method of particular solutions. *SIAM Review*,**47**, 469–491 (2005).

[CaHa12] Cakoni, F. and Haddar, H.: Transmission eigenvalues in inverse scattering theory. *Inside Out II*, **60**, 527–578 (2012).

[GiPa13] Cakoni, F., and Haddar, H.: Gintides, D. and Pallikaraki, N. A computational method for the inverse transmission eigenvalue problem. *Inverse Problems*, **29**, 104010 (2013).

[KiGr08] Kirsch A. and Grinberg N.: The Factorization Method for Inverse Problems. *Oxford University Press*, (2008).

[KlPi18a] Kleefeld, A. and Pieronek, L.: The method of fundamental solutions for computing acoustic interior transmission eigenvalues. *Inverse Problems*, **34**, 035007 (2018).

[KlPi18b] Kleefeld, A. and Pieronek, L.: Computing interior transmission eigenvalues for homogeneous and anisotropic media. *Inverse Problems*, **34**, 105007 (2018).